

Supporting Information

A Mn-54 radiotracer study of Mn isotope solid-liquid exchange during
reductive transformation of vernadite ($\delta\text{-MnO}_2$) by aqueous Mn(II)

Evert J. Elzinga^{*} and Adam B. Kustka

Department of Earth & Environmental Sciences, Rutgers University, Newark, NJ, USA

* Corresponding author. Email: elzinga@rutgers.edu; phone: (973) 353 5238

12 pages, 4 figures

1. Experimental protocols to ensure anoxic conditions

Anoxic experiments were performed using protocols described in Elzinga¹ and Lefkowitz et al.²

The experiments were carried out in an anaerobic chamber with a 95% N₂-5% H₂ atmosphere, and equipped with a Palladium catalyst (Coy Laboratories) for removal of trace atmospheric oxygen. Anoxic samples and reagents were prepared with anoxic DDI water, prepared by boiling under an N₂ atmosphere and cooling inside the glovebag. All labware used for the experiments (containers, centrifuge tubes, pipette tips, filters, etc.) was placed in the glovebag for at least 24 h before use.

2. Plot of [Mn(II)]_{aq} and [⁵⁴Mn(II)]_{aq} versus time, expressed as fractions of total added

Mn(II) and total ⁵⁴Mn

Figure S1 plots the same data as presented in Figure 1 of the main manuscript, but with the concentrations of aqueous Mn(II) and aqueous ⁵⁴Mn(II) expressed as a fraction of total added Mn(II) (800 μM) for the results of experiment 3, and as a fraction of total ⁵⁴Mn used for the hot experiments (132 kBq L⁻¹) for the results of experiments 1 and 2. The total aqueous Mn(II) drops by approximately half over the course of reaction, as shown by the results of experiment 3, whereas approximately 1/3 of total ⁵⁴Mn is present in solution as ⁵⁴Mn(II) at the completion of both experiments 1 and 2.

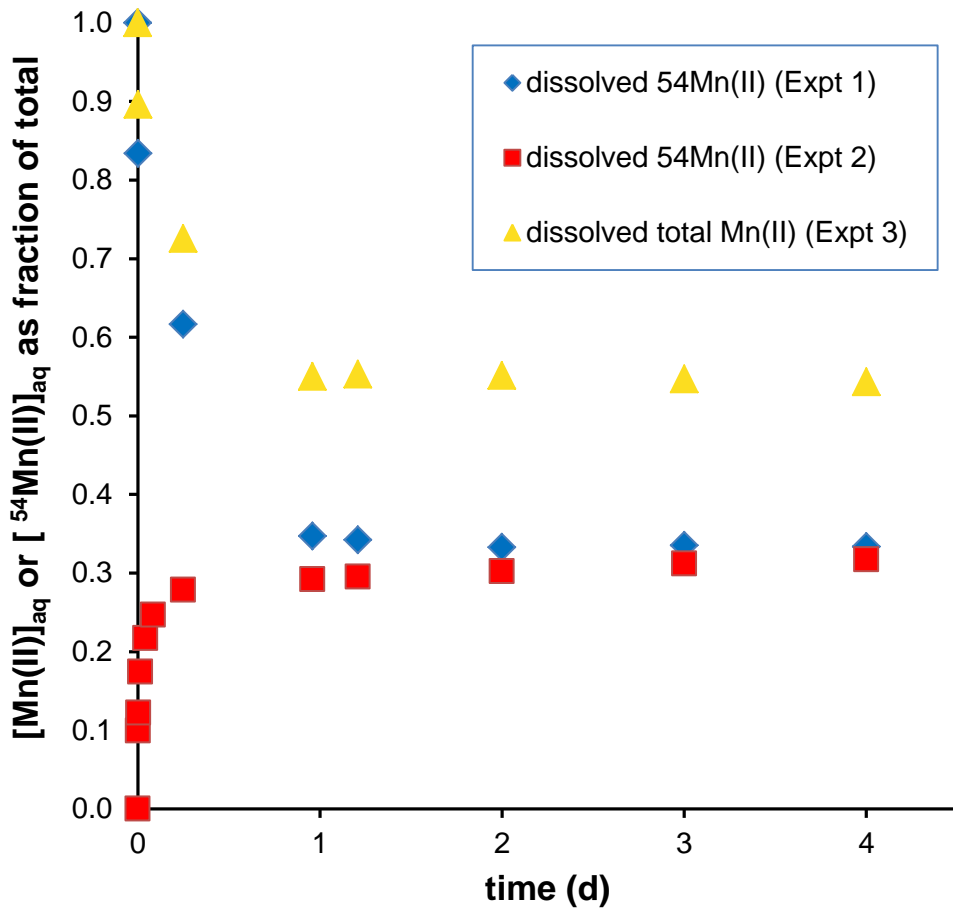


Figure S1. Time-dependence of the concentrations of $[{}^54\text{Mn(II)}]_{\text{aq}}$ in experiments 1 and 2, and of $[\text{Mn(II)}]_{\text{aq}}$ measured in experiment 3, expressed as a fraction of total added Mn(II) (800 μM) for the results of experiment 3; and as a fraction of total ${}^{54}\text{Mn}$ (132 kBq L^{-1}) for the results of experiments 1 and 2. The three experiments were conducted under identical conditions, using anoxic suspensions with a $\text{MnO}_{2(s)}$ or ${}^{54}\text{MnO}_{2(s)}$ particle loading of 530 μM , a pH of 7.5, and an initial $\text{Mn(II)}_{(\text{aq})}$ concentration of 800 μM .

3. Test of $\delta\text{-MnO}_2$ reactivity with HEPES buffer

Samples for powder XRD analyses were prepared inside the anaerobic glovebox from anoxic $\delta\text{-MnO}_2$ suspensions with the same suspension density (530 μM $\delta\text{-MnO}_{2(s)}$, corresponding to $\sim 0.05 \text{ g L}^{-1}$), the same background electrolyte (0.1 M NaCl) and the same pH (pH = 7.5) as used for the sorption experiments described in the main manuscript. Two samples were prepared in parallel.

In the first, HEPES buffer was added to the background electrolyte at a concentration of 25 mM to maintain pH at 7.5; this sample is identical to the $\delta\text{-MnO}_{2(s)}$ suspensions of the sorption experiments described in the main manuscript. The second sample contained no HEPES buffer, but instead was titrated to a pH value of 7.5 through manual addition of 0.05 M NaOH. The suspension pH was measured three times in the first 5 hours following initial titration and re-adjusted to pH 7.5 as necessary; the pH did not fall below values of 7.3 during this time period and was found to be stable at a pH value of 7.5 afterward.

In contrast to the sorption samples described in the main manuscript, the two samples prepared here received no aqueous Mn(II) but instead were equilibrated in their respective background electrolytes for 2 days. After 2 days, the samples were filtered inside the glovebox, and then washed and dried for analysis by powder X-ray diffraction (XRD) and synchrotron X-ray absorption spectroscopy (XAS). For XRD analysis, the dried powders were loaded onto low background sample holders and analyzed on a Bruker D8 Advance diffractometer using Ni-filtered Cu K α radiation and a LynxEye XE detector. For XAS analysis, samples were dispersed in boron nitride and analyzed in transmission mode at the Mn K -edge (6539 eV) on beamline 12BM-B of the Advanced Photon Source at Argonne National Laboratory. Processing of the XAS data was performed in WinXAS3.1³ using standard procedures.⁴

Figure S2 displays the normalized near-edge XAS spectra of the two vernadite samples. The spectrum collected for the sample hydrated in the presence of HEPES exhibits a slight shift in the edge position to lower energy and increased spectral intensity in the energy range 6.545-6.560 keV as compared to the sample hydrated in background electrolyte without HEPES (Figure S2). This difference demonstrates a higher content of reduced Mn(II) and/or Mn(III) in the vernadite substrate hydrated with HEPES. Since the only difference between the samples is

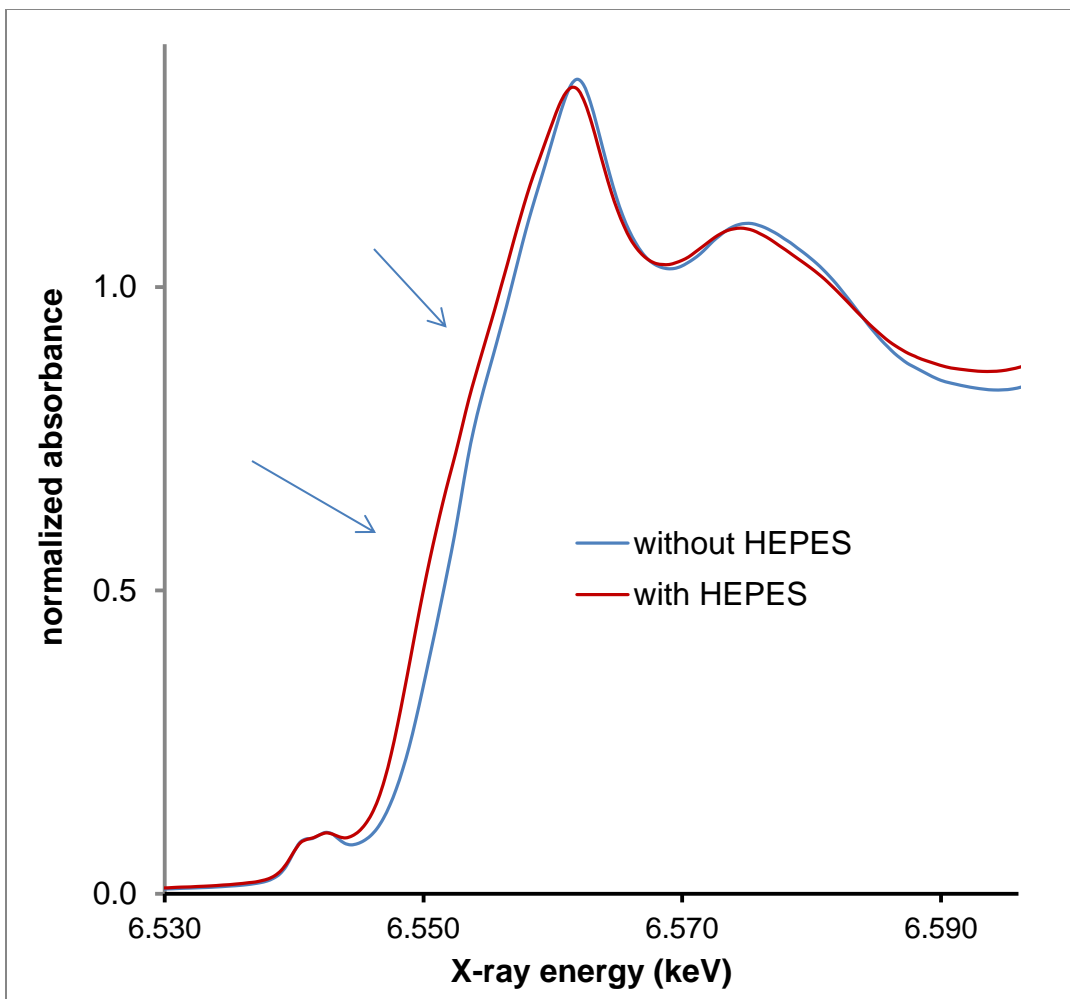


Figure S2. Manganese *K*-edge XAS spectra of $\delta\text{-MnO}_2$ solids following 2 days of hydration in anoxic 0.1 M NaCl background electrolyte at a suspension density of 530 μM and pH 7.5 in the absence or presence of 25 mM HEPES buffer. The slight shift in edge position and increased spectral intensity in the energy range 6.545–6.560 keV (pointed out by the arrows) in the spectrum of the HEPES-reacted sample demonstrate increased content of reduced Mn(II) and/or Mn(III) consistent with partial reduction of structural Mn(IV) by the HEPES buffer.

the presence of HEPES buffer, we attribute the presence of Mn(II, III) in the HEPES-reacted sample to partial reduction of structural Mn(IV) by the buffer.

Structural modification of vernadite during hydration with HEPES is evident from the results of powder XRD analyses presented in Figure S3, which shows the diffraction patterns of the two hydrated samples and that of the $\delta\text{-MnO}_2$ starting substrate. Consistent with previous

results,^{e.g. 5-8} the vernadite XRD pattern shows broad diffraction peaks at d-spacings near 2.4 and 1.4 Å, which are due to (20, 11) and (31, 02) reflections,⁵⁻¹¹ while 001 and 002 reflections (which occur near 7.2 and 3.6 Å in hexagonal birnessite) are absent due to the lack of long-range ordered sheet stacking in vernadite.⁵⁻⁹ The XRD pattern of $\delta\text{-MnO}_2\text{(s)}$ hydrated in background electrolyte without HEPES is essentially identical to that of the starting material (Figure S3a), which indicates that the material has remained unchanged during the 2 day hydration period. In contrast, the material hydrated in the presence of HEPES has undergone significant structural modifications. The XRD pattern shows pronounced new reflections at 7.1 and 3.6 Å (Figure

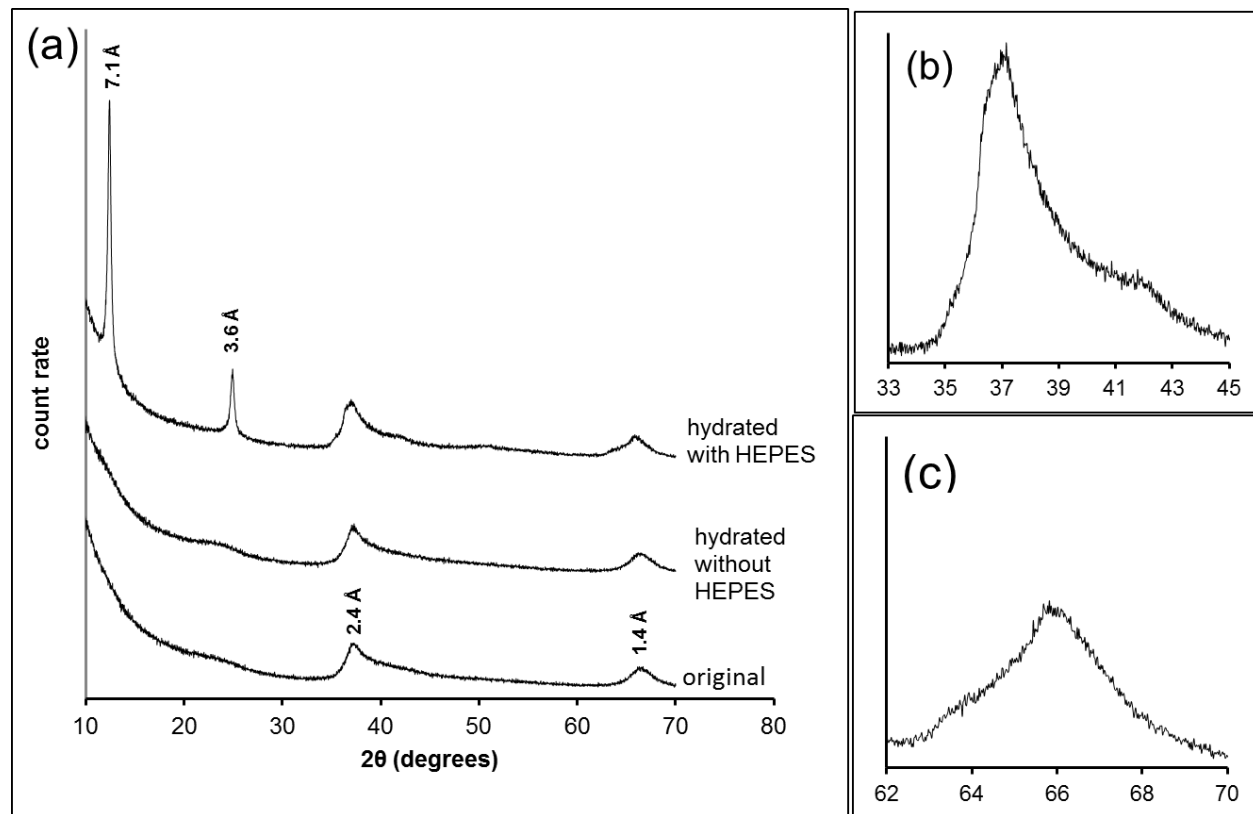


Figure S3. Powder X-ray diffraction (XRD) patterns of the original vernadite substrate and of the $\delta\text{-MnO}_2$ materials hydrated in anoxic 0.1 M NaCl background electrolyte at pH 7.5 in the absence or presence of 25 mM HEPES buffer. Panel (a) shows the full patterns collected for the three samples, while panels (b) and (c) are zoom-in of the (20, 11) and (31, 02) reflections, respectively, of the HEPES-reacted material.

S3a), demonstrating that the stacking order along the c-axis has increased. In addition, the (20, 11) and (31, 02) reflections of this samples exhibit distinct splitting (Figure S3b and c), which is indicative of a change in layer sheet symmetry from hexagonal to orthogonal or triclinic.⁹⁻¹¹ These structural changes are attributed to the partial reduction of the δ-MnO₂ substrate by HEPES evident from the XAS data (Figure S2). The change in octahedral layer symmetry suggests incorporation of Mn(III) into vacancy sites generating a Mn(III)-enriched phyllo manganese with structural similarities to triclinic birnessite, which is a phyllo manganese composed of vacancy-free octahedral sheets where 2/3 of structural Mn is present as Mn(IV) and the remaining 1/3 as Mn(III).^{7, 12, 13} Increased ordering of sheet stacking along c is attributed to migration of Mn(II) and/or Mn(III) cations into the interlayer region, where they displace weakly held Na⁺ as charge balancing cations, and mediate a higher degree of oriented sheet stacking through their relatively strong interactions with the phyllo manganese surface.

The results presented in Figures S2 and S3 are consistent with previous studies reporting redox reactivity of HEPES and related Good's buffers,¹⁴⁻¹⁸ which has been attributed to piperazine moieties on the buffer molecules. The ubiquitous use of Good's buffers as supposedly inert compounds in aqueous geochemical studies necessitates careful consideration of potential artifacts induced by these compounds in redox sensitive experiments.

4. Impact of HEPES on ⁵⁴Mn solid-liquid exchange during interaction of Mn(II)_(aq) with ⁵⁴MnO_{2(s)}

Due to the redox reactivity of HEPES toward δ-MnO_{2(s)} evident from the results presented above, we decided to check whether the presence of this compound in our experimental systems impacted our primary experimental finding, i.e. the rapid and quantitative exchange of Mn atoms between the solid and aqueous phase during interaction of Mn(II) with δ-MnO_{2(s)} at pH 7.5,

mediated by interfacial electron transfer reactions. To this end, we compared the results of two experiments, the first employing a HEPES-buffered suspension and the second a suspension where pH was controlled manually, which were run under otherwise identical conditions. The experiments were run side by side in an anaerobic glove bag using the same experimental parameters as in the sorption experiments described in the main manuscript, (i.e. 530 μ M vernadite suspension density, 0.1 M NaCl background, and a 800 μ M initial Mn(II) solution concentration). The experiments were conducted with ^{54}Mn -labeled $\delta\text{-MnO}_{2(\text{s})}$ (referred to as $^{54}\text{MnO}_{2(\text{s})}$) to monitor release of $^{54}\text{Mn(II)}_{(\text{aq})}$ into solution during reaction of $\text{Mn(II)}_{(\text{aq})}$ with the $^{54}\text{MnO}_{2(\text{s})}$ solid in the first 2 hours following $\text{Mn(II)}_{(\text{aq})}$ addition. The HEPES-buffered system was identical to that described in the main manuscript, whereas pH in the unbuffered system was maintained in the range of pH 7.30-7.50 by regular manual additions of small amounts of (anoxic) 0.05 M NaOH. The vessels were sampled prior to and at four time points (4, 15, 60 and 120 minutes) after the addition of cold Mn(II) to the $^{54}\text{MnO}_2$ suspension. Sampling involved filtration of a 5 mL subsample through a 0.2 μ m nitrocellulose membrane. The filtered reaction electrolytes were counted for the activity of dissolved $^{54}\text{Mn(II)}_{(\text{aq})}$ using the same methods as described in the main manuscript. Blank samples, made in the same way as the sorption samples except for the addition of $^{54}\text{MnO}_{2(\text{s})}$, and control samples, consisting of $^{54}\text{MnO}_{2(\text{s})}$ suspensions identical to those of the sorption experiments but without added Mn(II), were analyzed as well.

The results of these experiments are compared in Figure S4, which shows the build-up of $[^{54}\text{Mn(II)}]_{\text{aq}}$ in solution following addition of $\text{Mn(II)}_{(\text{aq})}$ at t=0, with $[^{54}\text{Mn(II)}]_{\text{aq}}$ quantified as the fraction of total ^{54}Mn in the system (132 kBq L^{-1}). The experimental results of the two systems are remarkably similar, showing quick and substantive appearance of $^{54}\text{Mn(II)}_{(\text{aq})}$ in solution following the addition of $\text{Mn(II)}_{(\text{aq})}$ (Figure S4). After 2 hours of reaction, 25% of total ^{54}Mn has

been released from the solid phase into solution in both systems, while 75% remains partitioned to the solid phase. Considering that the final (equilibrium) partitioning of ^{54}Mn involves 1/3 of total ^{54}Mn partitioned to solution as dissolved $^{54}\text{Mn}(\text{II})$ and 2/3 partitioned to the solid phase Mn-oxide as structural $^{54}\text{Mn}(\text{III}, \text{IV})$ (see Figure 1 of the main manuscript and Figure S1), these results indicate that the majority ($25/33 * 100 = 76\%$) of total ^{54}Mn solid-liquid exchange occurs within the first few hours of interaction, consistent with rapid establishment of dynamic equilibrium. The absence of a discernible impact of the presence of HEPES on these exchange reactions in this early reaction stage (Figure S4) suggests that $\text{Mn}(\text{II})\text{-Mn}(\text{IV})\text{O}_2$ surface interactions and the resulting exchange of Mn isotopes between the aqueous and solid phase

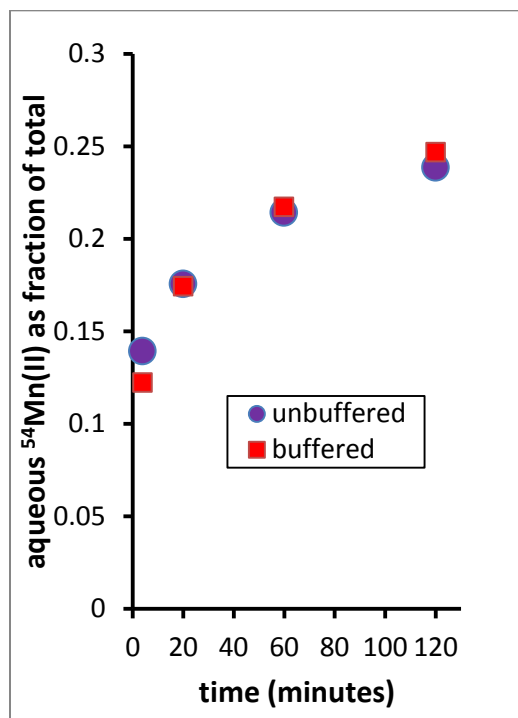


Figure S4. Release of $^{54}\text{Mn}(\text{II})_{(\text{aq})}$ release into solution during reaction of ^{54}Mn -labeled $\delta\text{-MnO}_{2(\text{s})}$ at pH 7.5 in the first 2 hours following $\text{Mn}(\text{II})_{(\text{aq})}$ addition (800 μM) in a HEPES-buffered suspension (red data points) and in an unbuffered suspension where pH was maintained through regular manual addition of 0.05 M NaOH aliquots (blue data). The $^{54}\text{MnO}_{2(\text{s})}$ suspension density was 530 μM in both experiments, and the samples were run under anoxic conditions. The four data points from the HEPES-buffered system are included in Figure 1 of the main manuscript as well, where they are presented along with the datapoints collected for an identical but separate experiment.

are not significantly affected by HEPES redox reactivity with MnO₂. Most importantly, the rapid release of ⁵⁴Mn(II) to solution observed in the HEPES-free system upon addition of cold Mn(II) to the ⁵⁴MnO₂ suspension confirms that our primary experimental finding, which is the rapid and extensive exchange of Mn atoms between aqueous Mn(II) and solid phase Mn(IV, III) indeed is mediated by interfacial electron transfer reactions between adsorbed Mn(II) and structural Mn(IV), and is not an experimental artifact associated with the presence of redox-active HEPES buffer in our samples.

REFERENCES

- (1) Elzinga, E. J. Reductive transformation of birnessite by aqueous Mn(II). *Environ. Sci. Technol.* **2011**, *45*, 6366–6372.
- (2) Lefkowitz, J. P.; Rouff, A.A.; Elzinga, E. J. Influence of pH on the reductive transformation of birnessite by aqueous Mn(II). *Environ. Sci. Technol.* **2013**, *47*, 10364–10371.
- (3) Rad, S.; Chemic, P.; Ressler, T. WinXAS: a program for X-ray absorption spectroscopy data analysis under MS-Windows. *J. Synchrotron Radiat.* **1998**, *5*, 118–122.
- (4) Fendorf, S. E., Sparks, D. L, Lambe, G. M, Kelley, M. J. Applications of x-ray absorption fine-structure spectroscopy to soils. *Soil Sci. Soc. Am. J.* **1994**, *58*, 1583–1595.
- (5) Villalobos, M.; Toner, B.; Bargar, J. R.; Sposito, G. Characterization of the manganese oxide produced by *Pseudomonas putida* strain MnB1. *Geochim. Cosmochim. Acta*. **2003**, *67*, 2649–2662.
- (6) Villalobos, M.; Lanson, B.; Manceau, A.; Toner, B.; Sposito, G. Structural model for the biogenic Mn oxide produced by *Pseudomonas putida*. *Am. Mineral.* **2006**, *91*, 489–502.

- (7) Drits, V.A.; Silvester, E.; Gorshkov, A.I.; Manceau, A. Structure of synthetic monoclinic Na-rich birnessite and hexagonal birnessite. 1. Results from X-ray diffraction and selected-area electron diffraction. *Am. Mineralogist* **1997**, *82*, 946-961.
- (8) Grangeon, A.; Lanson, B.; Lanson, M.; Manceau, A. Crystal structure of Ni-sorbed synthetic vernadite: A powder X-ray diffraction study. *Mineral Magazine*, **2008**, *72*, 1279-1291.
- (9) Drits, V.A.; Lanson, B.; Gaillot, A.C. Birnessite polytype systematics and identification by powder X-ray diffraction. *Am. Mineral.* **2007**, *92*, 771-788.
- (10) Webb, S.; Tebo, B.; Bargar, J., Structural characterization of biogenic Mn oxides produced in seawater by the marine *bacillus sp.* strain SG-1. *Am. Mineral.* **2005**, *90*, 1342-1357.
- (11) Zhu, M.; Ginder-Vogel, M.; Parikh, S. J.; Feng, X.-H.; Sparks, D. L., Cation effects on the layer structure of biogenic Mn-oxides. *Environ Sci. Technol.* **2010**, *44*, 4465-4471
- (12) Lanson, B.; Drits, V.A.; Feng, Q.; Manceau, A. Structure of synthetic Na-birnessite: Evidence for a triclinic one-layer unit cell. *Am. Mineral.* **2002**, *87*, 1662-1671.
- (13) Manceau, A.; Tommaseo, C.; Rihs, S.; Geoffroy, N.; Chateigner, D.; Schlegel, M.; Tisserand, D.; Marcus, M.A.; Tamura, N.; Chen, Z.-S. Natural speciation of Mn, Ni, and Zn at the micrometer scale in a clayey paddy soil using X-ray fluorescence, absorption, and diffraction. *Geochim. Cosmochim. Acta*, **2005**, *69*, 4007-4034.
- (14) Wang, F.; Sayre, L.M. Oxidation of tertiary amine buffers by copper(II). *Inorg. Chem.* **1989**, *28*, 169-170.
- (15) Hegetschweiler, K; Saltman, P. Interaction of copper(II) with N-(2-hydroxyethyl)piperazine-N'-ethanesulfonic acid (HEPES). *Inorg. Chem.* **1986**, *25*, 107-109.
- (16) Zhao, G; Chasteen, N.D. Oxidation of Good's buffers by hydrogen peroxide. *Anal. Biochem.* **2006**, *349*, 262-267.

- (17) Kirsch, M.; Lomonosova, E.E.; Korth, H.-G.; Sustmann, R.; de Groot, H. Hydrogen Peroxide Formation by Reaction of Peroxynitrite with HEPES and Related Tertiary Amines: Implications for a General Mechanism. *J. Biol. Chem.* **1998**, 273, 12716-12724.
- (18) Kostka, J. E.; Luther, G. W.; Nealson, K. H. Chemical and biological reduction of Mn(III)-pyrophosphate complexes – Potential importance of dissolved Mn(III) as an environmental oxidant. *Geochim. Cosmochim. Acta.* **1995**, 59, 885–894.